IISN 0379-301X

UNIVERSITE LIBRE DE BRUXELLES - VRIJE UNIVERSITEIT BRUSSEL

INTER-UNIVERSITY INSTITUTE FOR HIGH ENERGIES

COHERENT PRODUCTION OF A_1^- MESONS BY ANTINEUTRINO SCATTERING ON NEON

M. ADERHOLZ, P.P. ALLPORT, N. ARMENISE, J.P. BATON, M. BERGGREN, W. BURKOT, M. CALICCHIO, E.F. CLAYTON, T. COGHEN, A.M. COOPER-SARKAR, O. ERRIQUEZ, J. GUY, P.O. HULTH, G.T. JONES, P. MARAGE, E. MATSINOS, M.M. MOBAYYEN, D.R.O. MORRISON, M. NEVEU, S. O'NEALE, J. SACTON, R.A. SANSUM, E. SIMOPOULOU, K. VARVELL, A. VAYAKI, W. VENUS, H. WACHSMUTH, S. WAINSTEIN, W. WITTEK

BEBC WA59 Collaboration

Paper submitted to the 13th Conference on Neutrino and Astrophysics, Boston, June 1988

Universities of Brussels (ULB-VUB)
Pleinlaan, 2
B- 1050 Brussel

June 1988
IIHE-88.07

COHERENT PRODUCTION OF A_1^- MESONS

BY ANTINEUTRINO SCATTERING ON NEON.

M. ADERHOLZ[9], P.P. ALLPORT[10a], N. ARMENISE[1], J.P. BATON[12], M. BERGGREN[13b], W. BURKOT[8], M. CALICCHIO[1], E.F. CLAYTON[7], T. COGHEN[8], A.M. COOPER-SARKAR[11], O. ERRIQUEZ[1], J. GUY[11], P.O. HULTH[13], G.T. JONES[2], P. MARAGE[3], E. MATSINOS[5], M.M. MOBAYYEN[7], D.R.O. MORRISON[4], M. NEVEU[12], S. O'NEALE[2], J. SACTON[3], R.A. SANSUM[14a], E. SIMOPOULOU[5], K. VARVELL[2], A. VAYAKI[5], W. VENUS[11], H. WACHSMUTH[4], S. WAINSTEIN[7], W. WITTEK[9]

BEBC WA59 Collaboration

1 Dipartimento di Fisica dell'Università e Sezione INFN, I-70126 Bari, Italy
2 University of Birmingham, Birmingham, B15 2TT, UK
3 Inter-University Institute for High Energies, ULB-VUB, B-1050 Brussels, Belgium
4 CERN, CH-1211 Geneva 23, Switzerland
5 Nuclear Research Centre Demokritos, GR Athens, Greece
6 LPNHE, Ecole Polytechnique, F-91128 Palaiseau, France
7 Imperial College of Science and Technology, London, SW7 2AZ, UK
8 Institute of Nuclear Physics, PL-30055 Cracow, Poland
9 Max-Planck-Institut für Physik und Astrophysik, D-8000 München 40, Federal Republic of Germany
10 Department of Nuclear Physics, Oxford, OX1 3RH, UK
11 Rutherford Appleton Laboratory, Chilton, Didcot, OX11 0QX, UK
12 DPhPE, Centre d'Etudes Nucléaires, Saclay, F-91191 Gif-sur-Yvette, France
13 Institute of Physics, University of Stockholm, S-11346 Stockholm
14 Department of Physics and Astronomy, University College London, London WC1E 6BT, UK

a Now at Rutherford Appleton Laboratory
b Now at CERN

Paper submitted to the 13th Conference on Neutrino Physics and Astrophysics, Boston, June 1988

ABSTRACT.

Coherent production of A_1^- mesons in charged current antineutrino interactions on neon nuclei is studied in the bubble chamber BEBC exposed to the CERN SPS wide band beam. The absolute value of the cross section and the distributions of kinematical variables are in reasonable agreement with theoretical predictions based on the vector meson dominance model.

1. INTRODUCTION.

In this paper, we complete the study of channels contributing to antineutrino coherent scattering on neon nuclei in the Big European Bubble Chamber BEBC [1]. We study the process

$$\bar{\nu}\ Ne \rightarrow \mu^+ A_1^- Ne, \tag{1}$$

where the axial-vector part of the weak current, -dominated by the $J^{PC} = 1^{++}$ A_1 resonance-, coherently scatters off the neon nucleus, as illustrated in Fig. 1. The A_1 meson subsequently decays in a (ρ, π) system, giving -with equal branching ratios-

$$A_1 \rightarrow \rho^- \pi^\circ \rightarrow \pi^- \pi^\circ \pi^\circ \tag{1a}$$

$$A_1 \rightarrow \rho^\circ \pi^- \rightarrow \pi^- \pi^+ \pi^- \quad . \tag{1b}$$

In previous papers [2,3], we have studied the coherent production of π and ρ mesons :

$$\bar{\nu}\ Ne \rightarrow \mu^+ \pi^- Ne \tag{2}$$

$$\bar{\nu}\ Ne \rightarrow \mu^+ \rho^- Ne\ ;\quad \rho^- \rightarrow \pi^- \pi^\circ \quad . \tag{3}$$

These processes are due, respectively, to the coherent scattering off the nucleus of the scalar component of the axial-vector current (2) and of the vector current, dominated by the ρ meson (3).

The A_1 meson has been studied for a long time; its parameters and its very existence have long been controversial, at variance with its vector counter-part, the ρ meson. Indeed, ρ mesons are abundantly produced in diffractive scattering of photons, both real and virtual, in photo-, electro- and muoproduction :

$$\gamma\ p \rightarrow \rho^\circ\ p\ . \tag{4}$$

This process can be described in the framework of vector meson dominance models (VMD), where the electromagnetic current directly couples to vector particles. A similar production mode for the A_1 meson can only exist in neutrino scattering, since only the weak current contains an axial-vector

component :

$$\nu\ p \rightarrow \mu^-\ A_1^+\ p \rightarrow \mu^-\ \pi^+\ \pi^+\ \pi^-\ p. \qquad (5)$$

However, the observation of this production mode not only suffers from low statistics, but it is also obscured, in the case of diffractive scattering off protons, by the abundant production of $(\rho^\circ\ \Delta^{++})$ systems :

$$\nu\ p \rightarrow \mu^-\ \rho^\circ\ \Delta^{++} \rightarrow \mu^-\ \pi^+\ \pi^+\ \pi^-\ p. \qquad (6)$$

Four A_1 candidate events over an estimated background of 9 events were reported by experiment [4], and experiment [5] only quoted an upper limit for A_1 production. Coherent production of A_1 mesons by process (1) does not have reaction (6) as background, but the only previously reported result is of low statistical significance : (13 ± 9) events [6].

A_1 meson production has mostly been studied in hadron experiments, by scattering of π mesons [7]. However, the A_1 production is obscured in this case by the "Deck mechanism" [8], which enhances the non-resonant 3 π background, and distorts the A_1 resonance shape through interference with the background, making the analysis model dependent. The preferred values for the parameters of the A_1 resonance as determined by those hadron experiments are [9]

$$m_A = (1275 \pm 28)\ \text{MeV},$$

$$\Gamma_A = (316 \pm 45)\ \text{MeV}\ . \qquad (7)$$

In recent years, A_1 mesons have been observed with good statistics in the decay of τ leptons produced in e^+e^- experiments [10]. In this channel, the Deck mechanism is not expected to play an important role, and the resonance is produced in a much cleaner way; the parameters obtained for the A_1 resonance in the experiment with the highest statistics [10a] are

$$m_A = (1050 \pm 11)\ \text{MeV}, \qquad \Gamma_A = (521 \pm 27)\ \text{MeV}\ ; \qquad (8)$$

[10b] gives very similar results, whereas the use of a different

parametrization for the decay matrix of the τ lepton [10c] gives a higher mass value.

In the present analysis, we will use the parameters (8) in the expressions describing reaction (1); this will provide a test of the vector meson dominance model in the case of the axial-vector current, and a measure of the coupling constant between the A_1 meson and the weak axial-vector current.

2. EXPERIMENTAL DATA.

The data come from 16497 charged current antineutrino interactions collected from BEBC, filled with a 75 mole % Ne-H_2 mixture and exposed to the CERN SPS wide-band beam; muons are identified in the external muon identifier (EMI), and their momentum is required to exceed 5 GeV. This data sample was fully measured.

The final states which will be considered in the following and contribute to reaction (1) are

$$\mu^+ \pi^- \pi^\circ \pi^\circ \text{ Ne} \qquad (9a)$$

$$\mu^+ \pi^- \pi^\circ \gamma \text{ Ne} \qquad (9b)$$

$$\mu^+ \pi^- \pi^+ \pi^- \text{ Ne} \; ; \qquad (9c)$$

the final state (9b) corresponds to channel (1a) with one gamma lost; it is included in order to increase the statistics in that channel.

To achieve an efficient and reliable gamma detection, the events with 2 and 4 charged secondaries (2 and 4 prongs) were carefully rescanned; newly found gammas were measured and added to the events; bremsstrahlung gammas were discarded according to our usual procedure [11]. The overall detection efficiency deduced from the gamma multiplicity distribution among 2-prong events is (0.77 ± 0.04).

As in the case of the 2-prong events with 2 γ's [3], the (γ,γ) mass distribution for events with 3 and 4 gammas shows a clear π°

peak (Fig. 2a). The π^o fit probability distribution is flat above 1 % (Fig. 2b), and hereafter only combinations with probability higher than 1 % will be considered as π^o. It has been checked that the number of reconstructed π^o's among the 2-prong events with 3 or 4 γ's is in agreement with the quoted γ detection efficiency and with the estimated numbers of events with 2, 3 or 4 π^o's produced.

The procedure to extract the coherent signal has been described in [1]. Coherent events have an even number of prongs, since the recoil nucleus is not detected in the bubble chamber; there are no boil-off protons or nuclear fragments, due to the fact that the nucleus recoils as a whole, without breakup; those events have an exponentially falling t-distribution, t being the square of the 4-momentum transfer to the nucleus (see Fig. 1). For diffractive events, $|t|$ can be approximated as

$$|t| = [\sum_i (E_i - p_i'')]^2 + |\sum_i \vec{p}_i^T|^2 \quad , \qquad (10)$$

where E_i, p_i'' and $\vec{p}_i^T$ are, respectively, the energy, the longitudinal momentum and the transverse momentum of particle i with respect to the neutrino beam direction, the sum extending over all final state particles.

In this experiment, it is possible to identify protons stopping in the bubble chamber, with momentum up to ~ 1 GeV. All events were rescanned for the presence of protons or nuclear fragments at the vertex, indicating that the interaction was not coherent. In previous papers [1-3], the sample of non-coherent events used for background studies consisted of events with an even number of prongs, -i.e. interactions on neutrons-, containing nuclear fragments or protons with momentum below 300 MeV, called "stubs"; the stubs are not taken into account to compute the kinematical quantities of the event. In the case of channels (9a-c), however, the number of such events is small (respectively 10, 22 and 57). In order to increase the statistical significance of the background studies, we follow thus here the procedure used in our study of coherent π^+ production by neutrinos [12] : interactions on protons of type $\mu^+ \pi^- \pi^o \pi^o p$, $\mu^+ \pi^- \pi^o \gamma p$ and $\mu^+ \pi^- \pi^+ \pi^- p$ (with or without stubs with momentum below 300 MeV) are included in the sample of non-coherent events, the proton being discarded to compute the kinematical variables; those events are widely called "events with stubs".

Extending the definition (10) of $|t|$ to non-coherent events, the $|t|$-distributions of events with and without stubs can be compared. As noted in [1], the $|t|$-distributions at low $|t|$-values are similar for those two classes in the case of 3- and 5-prong events, -which are all necessarily non-coherent; it has been checked that this remains true with the extended definition of "stubs" used here. This indicates that the events with stubs provide a good description of the shape of the $|t|$-distribution of all the incoherent events.

For a given $|t|$-upper limit, the coherent signal is obtained from the excess of events without stub at lower $|t|$-values, above an incoherent background; this background is given by the number of events with stubs below the $|t|$-cut, weighted by a normalisation factor which is the ratio of the number of events without stub to the number of events with stubs, above the $|t|$-cut.

The $|t|$-distributions for the events corresponding to the final states (9a-c) are shown on Fig. 3; the signal is also given in Table 1 for several $|t|$ upper limits. It is interesting to note that the requirement of π° fits in the events with 3 and 4 γ's does not change the size of the signal : at $|t| < 0.15$ GeV^2, it is (16 ± 6) events both for the $(\mu^+ \pi^- 4\gamma) + (\mu^+ \pi^- 3\gamma)$ events, and for the $(\mu^+ \pi^- \pi^\circ \pi^\circ) + (\mu^+ \pi^- \pi^\circ \gamma)$ events.

$\|t\|$ upper limit (GeV^2)	0.05	0.10	0.15	0.20	0.25	∞
$\mu^+ \pi^- \pi^o \pi^o$						
ev. without stub	2	9	12	16	19	30
ev. with stubs	1	2	3	5	8	25
signal	0.8	7.2	9.6	12.5	13.8	
error on signal	±1.9	±3.3	±3.8	±4.5	±5.1	
$\mu^+ \pi^- \pi^o \gamma$						
ev. without stub	4	8	12	17	18	41
ev. with stubs	1	4	9	11	15	56
signal	3.3	5.5	6.5	11.1	9.6	
error on signal	±2.1	±3.2	±4.1	±4.7	±5.3	
$\mu^+ \pi^- \pi^+ \pi^-$						
ev. without stub	9	21	29	37	44	125
ev. with stubs	3	8	22	27	40	211
signal	7.3	16.9	17.8	24.1	25.0	
error on signal	±3.2	±4.8	±6.0	±6.8	±7.7	

Table 1 : Number of events with and without stubs, and excess of events with no stub at low $|t|$-values above the incoherent background obtained from the scaling of the number of events with stubs, for several $|t|$ upper limits and for the final states (9) relevant for the A_1 coherent production.

3. THEORETICAL PREDICTIONS.

The cross section for coherent diffractive production of A_1 mesons by the diagram of Fig. 1(*) is [13] :

$$\frac{d^3\sigma}{dQ^2\, d\nu\, dt} = \frac{G^2}{4\pi^2} f_A^2 \left(\frac{1}{Q^2+m_A^2}\right)^2 Q^2 \frac{\nu}{E_{\bar{\nu}}^2} \frac{1}{1-\varepsilon}$$

$$.(1+\varepsilon R) \frac{d\sigma^T (A_1^- Ne \rightarrow A_1^- Ne)}{dt} , \qquad (11)$$

where $G = 1.166\ 10^{-5}\ GeV^{-2}$ is the weak coupling constant, $f_A = C_A\, m_A^2$ is the coupling constant of the A_1 meson to the intermediate W boson; m_A is the A_1 meson mass (8); Q^2 is the square of the 4-momentum transfer from the leptons to the hadrons, $\nu = E_{\bar{\nu}} - E_{\mu^+}$;

$$\varepsilon = \frac{4\, E_{\bar{\nu}}\, (E_{\bar{\nu}} - \nu) - Q^2}{4\, E_{\bar{\nu}}\, (E_{\bar{\nu}} - \nu) + Q^2 + 2\nu^2} \qquad (12)$$

(*) The axial-vector component of the weak current contains also, according to the PCAC hypothesis, a term proportional to the gradient of the pion field; A_1 mesons can thus also be produced by diffractive scattering of virtual pions coupling directly to the scalar component of the weak axial current. However, this contribution to the cross section is negligible, being proportional to the final state lepton mass squared. On the other hand, a ρ meson could couple to the vector part of the W field, and produce an A_1 via pion exchange; however, such a process would transfer isospin to the nucleus, and would thus be inhibited in the case of coherent interactions with an isoscalar nucleus. We will thus not consider these contributions here (see similar discussion in [2]).

is the polarisation parameter of the virtual intermediate boson, and R is the ratio $\frac{d\sigma^L}{dt} / \frac{d\sigma^T}{dt}$, where σ^L and σ^T are, respectively, the longitudinal and the transverse (A_1 Ne) cross sections. As in the case of coherent ρ production, we will compare our data to the model predictions for

$$\text{(i)} \quad R = 0 \tag{13}$$

$$\text{(ii)} \quad R = 0.4\ Q^2 / m^2_A \quad , \ R <= 1 \ . \tag{14}$$

The axial-vector coupling constant f_A is not known experimentally; two possibilities have been proposed. In [15], the assumption is made that the decay width $A_1 \to \mu\ \nu$ is the same as that for the ρ meson, leading to

$$C^2_A = C^2_\rho\ m_\rho / m_A \ , \tag{15}$$

where $C^2_\rho = 2 / \gamma^2_\rho$, with $\gamma^2_\rho / 4\pi = 2.4$,

i.e. $f^2_A/f^2_\rho = 2.5$ for $m_A = 1.050$ GeV and $f^2_A/f^2_\rho = 4.5$ for $m_A = 1.275$ GeV.

In [16], one takes $f^2_A = f^2_\rho$:

$$C^2_A = C^2_\rho\ (m_\rho / m_A)^4 \ , \tag{16}$$

As in the case of coherent production of ρ meson , the A_1 Ne elastic cross section is given by

$$\frac{d\sigma\ (A_1^- \text{Ne} \to A_1^- \text{Ne})}{dt} = \frac{A^2}{16\pi}\ \sigma^2_{tot}\ (A_1^-\ N)\ e^{-b|t|}\ F_{abs}, \tag{17}$$

where A = 20 is the neon atomic number and $\sigma_{tot}\ (A_1^-\ N)$ is the total A_1^- nucleon cross section at $E_{A_1} = \nu$; in the absence of data, we take

$$\sigma(A_1^-\ N) = \sigma(\rho^-\ N) = \sigma\ (\pi^-\ N) \ , \tag{18}$$

as suggested by the additive quark model.

The slope parameter b is proportional to the transverse dimensions of the nucleus :

$$b = \alpha A^{2/3} , \tag{19}$$

and we take for α the value measured in coherent ρ^o photoproduction, as in [3] :

$$\alpha = (10.8 \pm 0.4)\ GeV^{-2},\ b = (80 \pm 3)\ GeV^{-2}. \tag{20}$$

The factor F_{abs} accounts for reinteractions of the A_1 meson and its decay products inside the nucleus; again we use, as in [3], experimental data obtained from coherent ρ^o photoproduction :

$$F_{abs} = 0.47 \pm 0.03. \tag{21}$$

4. TOTAL CROSS SECTION.

Table 2 presents the raw signal for reaction (1) for $|t| < 0.15\ GeV^2$ and the corrections to be applied on the data in order to determine the total cross section.

	$\mu^+ \pi^- \pi^o \pi^o$	$\mu^+ \pi^- \pi^o \gamma$	$\mu^+ \pi^- \pi^+ \pi^-$
raw signal (no. of ev.)	9.6 ± 3.8	6.5 ± 4.1	17.8 ± 6.0
correction factors for:			
undefined charge	1.08	1.08	1.25
scanning losses	(1.03 ± 0.02)		(1.03±0.02)
cut in $\|t\|$	(1.16±0.06)	(1.30±0.10)	(1.02±0.01)
γ detection eff.	(1.31 ± 0.11)		-
p_μ cut	1.23	1.23	1.23
corrected no. of events.	35.1 ± 12.6		28.8 ± 9.7

Table 2 : Raw and corrected numbers of coherent events

For this analysis, one has discarded the events in which a charged pion has interacted in the liquid so close to the vertex that its charge could not be reliably defined. The remaining events have been weighted accordingly, the weight depending on the charged prong multiplicity and on the total hadronic energy of the event; the average weights for the classes of events under study are presented in Table 2.

The scanning efficiencies for 2-prong events with gammas and for 4-prong events without gammas are both evaluated to be (97 ± 2) %.

A Monte-Carlo simulation based on (11)-(21) has been performed, taking into account the experimental resolution. This simulation has been used to evaluate the effects of the cuts in $|t|$ separately for the different final states (9). One observes that the $|t|$-distributions of the events containing π^o's are predicted to be broader than for the $\mu^+ \pi^- \pi^+ \pi^-$ events. This is due to the large measurement errors on the gamma's forming the π^o's, and to the occasional wrong gamma pairing in the π^o reconstruction; in addition, the loss of a γ affects the second term in (10), and contributes to broaden still more the $|t|$-distribution of the $\mu^+ \pi^- \pi^o \gamma$ events.

One has also to apply a weighting factor (1.31 ± 0.11) to the sum of the 2-prong final states (9a) and (9b), to take into account the gamma detection efficiency.

Finally, a common correction factor has to be applied to all final states (9) to account for the effect of the p_μ cut at 5 GeV; this factor is evaluated by the Monte-Carlo simulation to be 1.23.

The corrected number of events attributed to reaction (1) is thus (63.9 ± 15.9). The cross section for coherent A_1 meson production in antineutrino charged current interactions is found to be (91 ± 23). 10^{-40} cm^2 per neon nucleus, averaged over the SPS wide-band beam energy spectrum (above 15 GeV). This number is determined using the total number of charged current $\bar{\nu}$ interactions in the present experiment (taking into account a 4 % correction due to interactions on the H_2 in the liquid), and the known charged current antineutrino-nucleon cross section : $\sigma/E_{\bar{\nu}}$ = (0.35 ± 0.02) . 10^{-38} cm^2/GeV [18]. All the errors have been added in quadrature.

The absolute value for the cross section of coherent A_1 production in two energy bins ($15 < E_{\bar{\nu}} < 35$ GeV and $E_{\bar{\nu}} > 35$ GeV) is shown in Fig. 4, and is compared to the Monte-Carlo predictions based on (11) t (21).

A fair agreement is observed with the solid curve, which presents the prediction for the choice (15) of the A_1-W coupling, with $m_A = 1.050$ GeV (8) and R = 0 (12). Taking into account the errors on the slope b (20), the absorption factor F_{abs} (21) and the flux shape, the model predicts, for this choice of the parameters m_A and R, the observation of (30 ± 3) events in our experimental conditions and cuts, whereas (34 ± 8) events are seen. The predicted number is increased by some 35 % if one takes the value (14) for R, and decreased by about 5 % if $m_A = 1.275$ GeV (7) and R = 0, C_A^2 being modified according to (15).

On the other hand, only (12 ± 1) events are predicted if $f_A^2/f_\rho^2 = 1$ (16) (dashed curve on Fig. 4); this number falls to (6 ± 1) events if $m_A = 1.275$ GeV (for R = 0).

Using the predictions of the model (11)-(21), one finds thus, for R = 0,

$$f_A^2/f_\rho^2 = 2.9 \pm 0.7 \qquad (22)$$

$$f_A = (0.25 \pm 0.03)\ \text{GeV}^2 \qquad (23)$$

for $m_A = 1.050$ GeV, and

$$f_A^2/f_\rho^2 = 5.4 \pm 1.3 \qquad (24)$$

$$f_A = (0.34 \pm 0.04)\ \text{GeV}^2 \qquad (25)$$

for $m_A = 1.275$ GeV.

5. KINEMATICAL VARIABLES.

Fig. 5 a-i present the distributions of the coherent signal at $|t| < 0.15$ GeV^2 for the antineutrino energy $E_{\bar{\nu}}$, the energy transfer to the hadrons ν, the 4-momentum transfer to the hadrons Q^2, the Bjorken variables $x = Q^2/2 M_p \nu$ (M_p being the nucleon mass) and $y = \nu/E_{\bar{\nu}}$, the hadronic invariant mass $W = (2 M \nu - Q^2 + M_p^2)^{1/2}$, the 3-pion invariant mass $m(3\pi)$, the square of the 4-momentum transfer for the nucleus $|t|$, and the variable $t' = |t| - t_{min}$, where $t_{min} \sim [(Q^2 + m_A^2)/2 \nu]^2$; the events with stubs are given a negative weight corresponding to the background contribution to the different channels as obtained from Table 1 (respectively -0.82, -0.62 and -0.51); all events are weighted to correct for the loss of events with undefined charge. The average values for these variables are given in Table 3.

	Data	Model	
		m_A (GeV) 1.050	1.275
E_ν (GeV)	36.4 ± 5.3	43.5	46.4
P_μ (GeV)	21.2 ± 4.4	24.1	24.3
ν (GeV)	15.1 ± 3.2	19.4	22.1
Q^2 (GeV^2)	2.06 ± 0.59	1.81	1.96
x	0.076± 0.011	0.054	0.051
y	0.419± 0.052	0.458	0.488
W (GeV)	4.83 ± 0.47	5.55	5.96
$\|t\|$ (GeV^2)	0.064± 0.008	0.038	0.040
t' (GeV^2)	0.040± 0.008	0.028	0.029
$m(3\pi)$ (GeV)	1.098± 0.077	0.977	1.147

Table 3 : Mean values of kinematical variables for the coherent events, after background subtraction; they are compared to the predictions of the model (11) to (21), including the effects of experimental resolution, for two values of the mass m_A.

The Monte-Carlo predictions based on (11)-(21), with m_A = 1.050 GeV, Γ_A = 0.520 GeV (8) and R = 0 (13) are shown superimposed on the distributions in Fig. 5, and are also given in Table 3.

The general features of the data are reasonably well described by the model, especially if one compares the ν-, y- and Q^2-distributions with those for coherent pion production, where they are rapidly falling [2]; as expected, they have also higher average values than in the case of ρ production [3].

However, in detail there are discrepancies. The $|t|$-, t'- and x-distributions are flatter than expected, and the E_{ν}-, ν-, y-, and W-distributions are softer, whereas Q^2 is in good agreement with the expectation; all these features are kinematically related.

The strongest disagreement is in the $|t|$-distribution (Fig. 5h). The simulation fails to reproduce the maximum around 0.5 GeV^2, as seen in the data. Fig. 5h shows also the $|t|$-distribution above 0.15 GeV^2 : one observes an excess larger than expected of events without stub above the background up to $|t|$-values ~ 0.2 GeV^2.

Experimental effects explaining an apparent softening of the ν-distribution have been searched for. In fact, the average π^0 momentum in the $\mu^+ \pi^- \pi^0 \pi^0$ events [(3.3 ± 1.0) GeV] is lower than the corresponding π^- momentum in the $\mu^+ \pi^+ \pi^- \pi^-$ events [(4.9 ± 1.7) GeV]; an underestimation of the γ and π^0 momenta, or the loss of high energy gammas could thus partly explain the effect in ν. However, there is no direct evidence of such experimental effects and, in addition, the effect in ν is also observed among the 4-prong events [$\langle\nu\rangle$ = (15.9 ± 4.5) GeV instead of 21.5 GeV predicted]. It might be remembered that, in our study of the ρ^- coherent production in BEBC [3], the average ν-value was also (marginally) lower than predicted, and that a lack of high energy events was reported from a study of ρ coherent production in the 15' bubble chamber at FNAL [19].

The effect of varying some of the parameters in the model was also studied. Changing the A_1 mass from 1.050 GeV to 1.275 GeV has no significant effect on the $|t|$-, t'- and x-distributions; however,

$t_{min} \simeq \left(\frac{Q^2 + m_A^2}{2\nu}\right)^2$ is increased, and accordingly higher $E_{\bar{\nu}}$-, ν-, y- and W-values are predicted (see Table 3); the disagreement in these variables is thus stronger than with a lower mass value.

Choosing for R the values (14) instead of R = 0 has only a a minor effect on the differential distributions : only the Q^2 and x-value are slightly increased.

One could also suggest that the model does not really work at Q^2 values above a few GeV^2 [17]; however, cutting out the events with $Q^2 > 7\ GeV^2$ or even $Q^2 > 3\ GeV^2$ does not improve the agreement with the (modified) predictions.

6. CONCLUSIONS.

In conclusion, we have completed the study of the channels contributing to the signal of antineutrino coherent scattering on neon nuclei in BEBC, by the analysis of A_1 production in the channels

$$\bar{\nu}\ Ne \rightarrow \mu^+ \pi^- \pi^o \pi^o\ Ne$$

$$\bar{\nu}\ Ne \rightarrow \mu^+ \pi^- \pi^o \gamma\ Ne$$

$$\bar{\nu}\ Ne \rightarrow \mu^+ \pi^- \pi^+ \pi^-\ Ne.$$

The cross section for A_1 production, averaged over the SPS $\bar{\nu}_\mu$ wide band beam energy spectrum above 15 GeV is (91 +- 23). 10^{-40} cm^2 per neon nucleus. For a ratio of longitudinal to transverse cross sections R = 0, and for m_A = 1.050 GeV, this corresponds to an A_1- W coupling constant f_A = (0.25 ± 0.03) GeV^2, and to a ratio f^2_A/f^2_ρ = 2.9 ± 0.7. The kinematical distributions are in reasonable agreement with the vector meson model predictions, although the |t|- and x-distributions are flatter and the ν-distribution softer than expected.

Acknowledgements.

We express our gratitude to the CERN staff for excellent beam conditions and bubble chamber operation, and to the scanning and measuring staff in our institutions for their dedicated work.

REFERENCES.

[1] P. Marage et al. : Phys. Lett. 140B, 137 (1984)

[2] P. Marage et al. : Z. Phys. C - Particles and Fields 31, 191 (1986)

[3] P. Marage et al. : Z. Phys. C - Particles and Fields 35, 275 (1987)

[4] J. Bell et al. : Phys. Rev. Lett. 40, 1226 (1978)

[5] D.R.O. Morrison : Proc. of the 1978 Int. Meeting on Frontier of Physics, K.K. Phua, C.K. Chew and Y.K. Lim (eds.), Singapore National Academy of Science, 205 (1978)

[6] A. Bouchakour : Thesis, Strasbourg (1980), unpubl.

[7] see e.g. :
C. Daum et al. : Nucl. Phys. B182, 269 (1981)
J. Dankowych et al. : Phys. Rev. Lett. 46, 580 (1981)
and references therein

[8] R.T. Deck : Phys. Rev. Lett. 13, 169 (1964)

[9] The Particle Data Group, M. Aguilar Benitez et al. : Phys. Lett. B170, 1 (1986)

[10] a. H. Albrecht et al. (ARGUS Coll.) : Z. Phys. C - Particles and Fields 33, 7 (1986)
b. W. Rückstuhl et al. (DELCO Coll.) : Phys. Rev. Lett. 56, 2132 (1986)
c. W.B. Schmidke et al. (MARK II Coll.) : Phys. Rev. Lett. 57, 527 (1986)

[11] W. Wittek et al., WA59 Coll., Production of π^0 mesons and charged current hadrons in ν Neon and $\bar{\nu}$ Neon charged current interactions, MPI-PAE/Exp. EL 188, to be publ. in Z. Phys. C.

[12] P. Allport et al.; WA 59 Coll.; Coherent production of π^+ mesons in ν-neon interactions, subm. to the 13th Neutrino Conference, Boston 1988.

[13] The form of the cross-section has been given among others in ref. [14-17]; note however the comments in the footnote (20) of ref. [3]

[14] C.A. Piketty, L. Stodolsky : Nucl. Phys. B15, 571 (1970)

[15] M.K. Gaillard, S.A. Jackson, D.V. Nanopoulos : Nucl. Phys. B102, 326 (1976); Nucl. Phys. B112, 545 (1976)

[16] M.S. Chen, F.S. Henyey, G.L. Kane : Nucl. Phys. B118, 345 (1977)

[17] A. Bartl, H. Fraas, W. Majerotto : Phys. Rev. D16, 267 (1977)

[18] M. Aderholz et al. : Phys. Lett. 173B, 211 (1986)

[19] H. Bingham, Proc. of the 12th International Conference on Neutrino Physics and Astrophysics, Sendai 1986, p. 555.

FIGURE CAPTIONS.

Fig. 1. Coherent diffractive production of an A_1^- meson by $\bar{\nu}_\mu$ charged current interaction on a neon nucleus.

Fig. 2. Distributions of a. the ($\gamma\gamma$) mass; b. the π^o probability P (with P > 1 %), for the 2-prong events with 3 or 4 gammas (146 events).

Fig. 3a,b,c,d. Distribution of the square of the 4-momentum transfer |t| for the events without stub (full histogram) and the events with stubs (dashed histogram), for a. the ($\mu^+ \pi^- \pi^o \pi^o$) events; b. the ($\mu^+ \pi^- \pi^o \gamma$) events; c. the ($\mu^+ \pi^- \pi^+ \pi^-$) events; d. the 3 combined classes. The distribution for the events with stubs is normalised to that for the events without stub for $|t| > 0.15$ GeV^2.

Fig. 4. Cross section for coherent A_1 production by $\bar{\nu}_\mu$ charged current interactions on neon nuclei, as a function of the $\bar{\nu}$ energy $E_{\bar{\nu}}$; the curves are the predictions of the model (11) to (21) for m_A = 1.050 GeV (8), R = 0 (13) and the A_1-W coupling constant being taken as in (15) (solid curve) and as in (16) (dashed curve).

Fig. 5a-i. Distributions for a. $E_{\bar{\nu}}$; b. ν; c. Q^2; d. W; e. x; f. y; g. m(3π); h. |t|; i. t' for the combined channels (9a-c), with $|t| < 0.15$ GeV^2, weighted for the loss of events with undefined charge; the incoherent background, estimated from the events with stubs, is shown hatched. The curves, normalised to the coherent signal, are the predictions of the model (11) to (21), including the effects of experimental resolution, with m_A = 1.050 GeV, Γ_A = 0.520 GeV (8), and R = 0 (13).

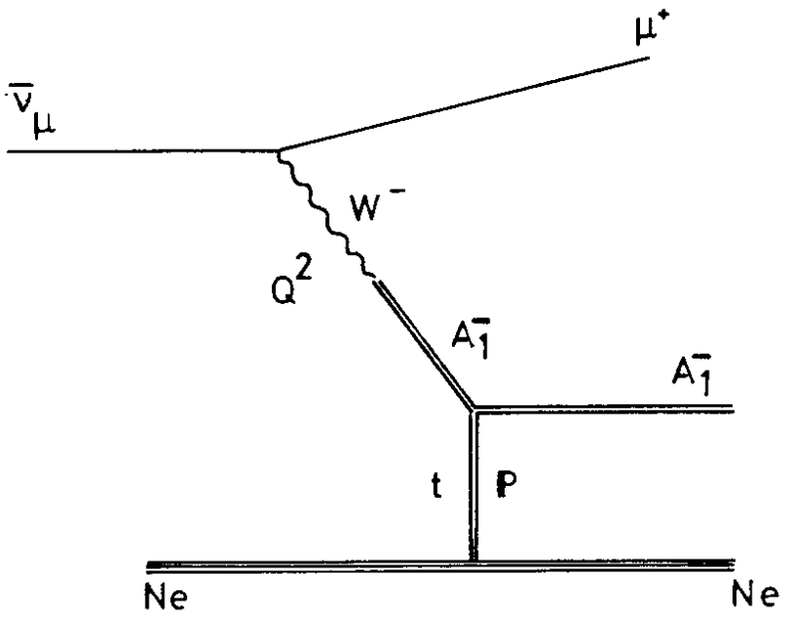

Fig. 1

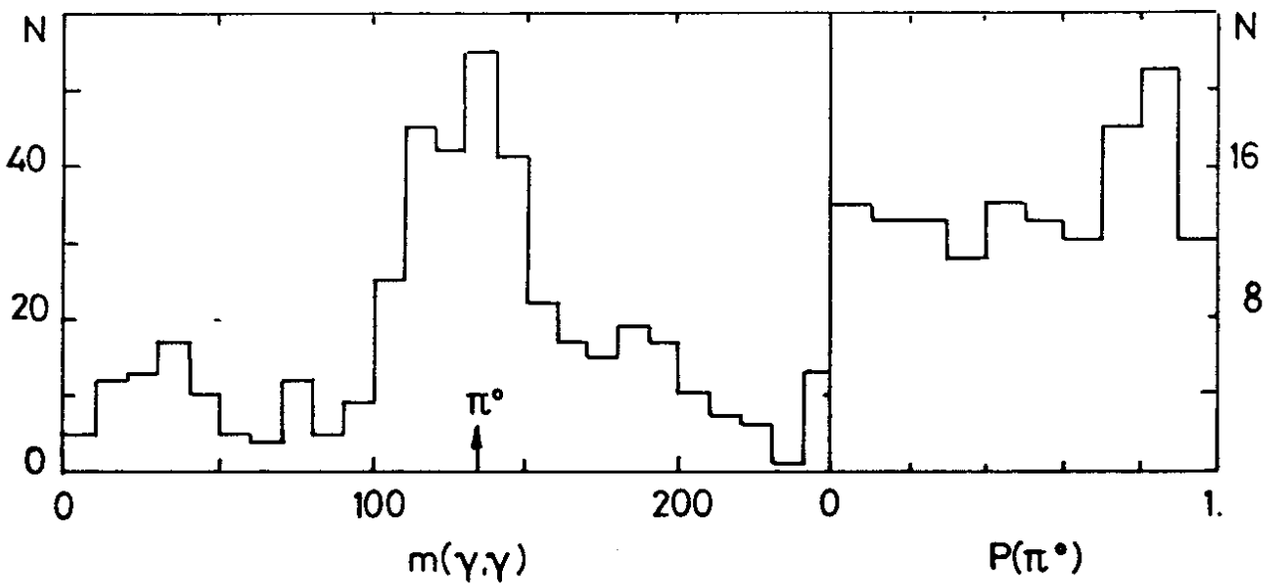

Fig. 2

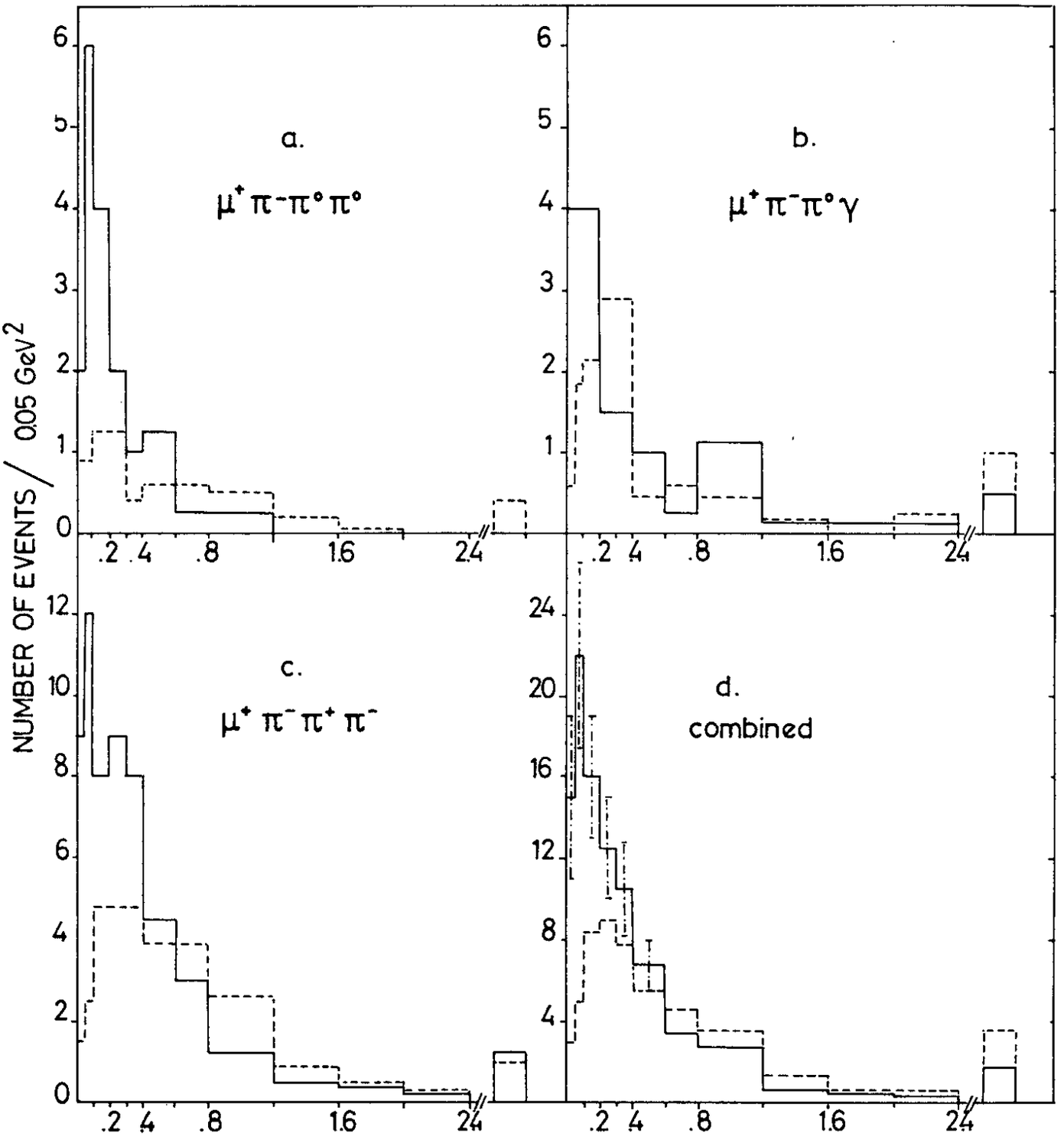
a.
$\mu^+\pi^-\pi^\circ\pi^\circ$
b.
$\mu^+\pi^-\pi^\circ\gamma$
c.
$\mu^+\pi^-\pi^+\pi^-$
d.
combined
NUMBER OF EVENTS / 0.05 GeV^2
.2
.4
.8
1.6
2.4

Fig. 3

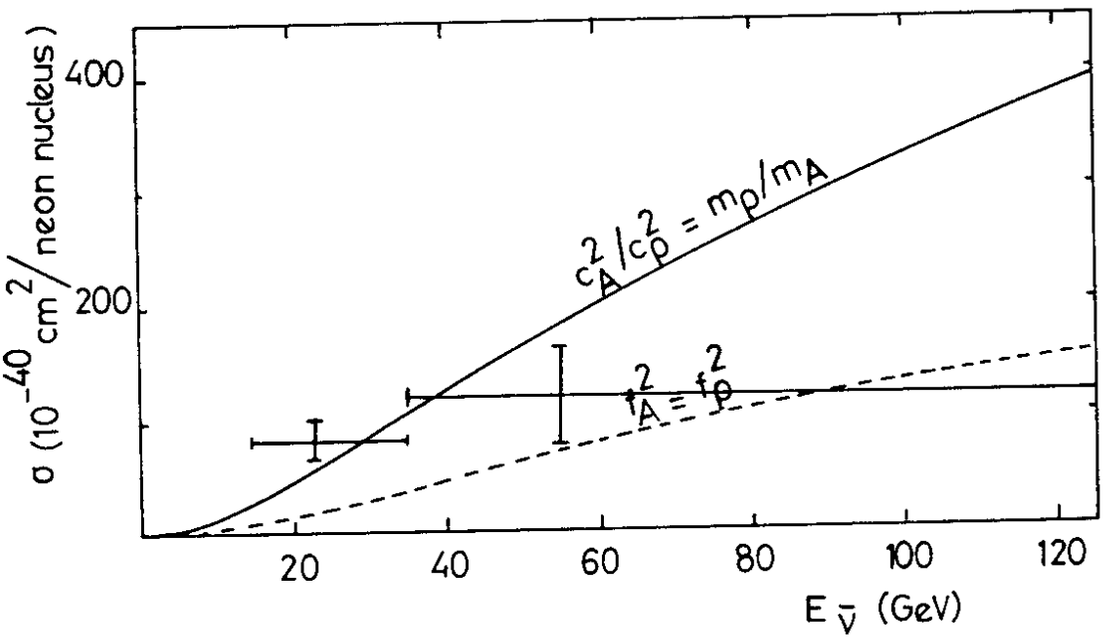
σ (10^-40 cm^2/neon nucleus)
400
200
20
40
60
80
100
120
E ν̄ (GeV)
c_A^2/c_p^2 = m_p/m_A
f_A^2 = f_p^2

Fig. 4

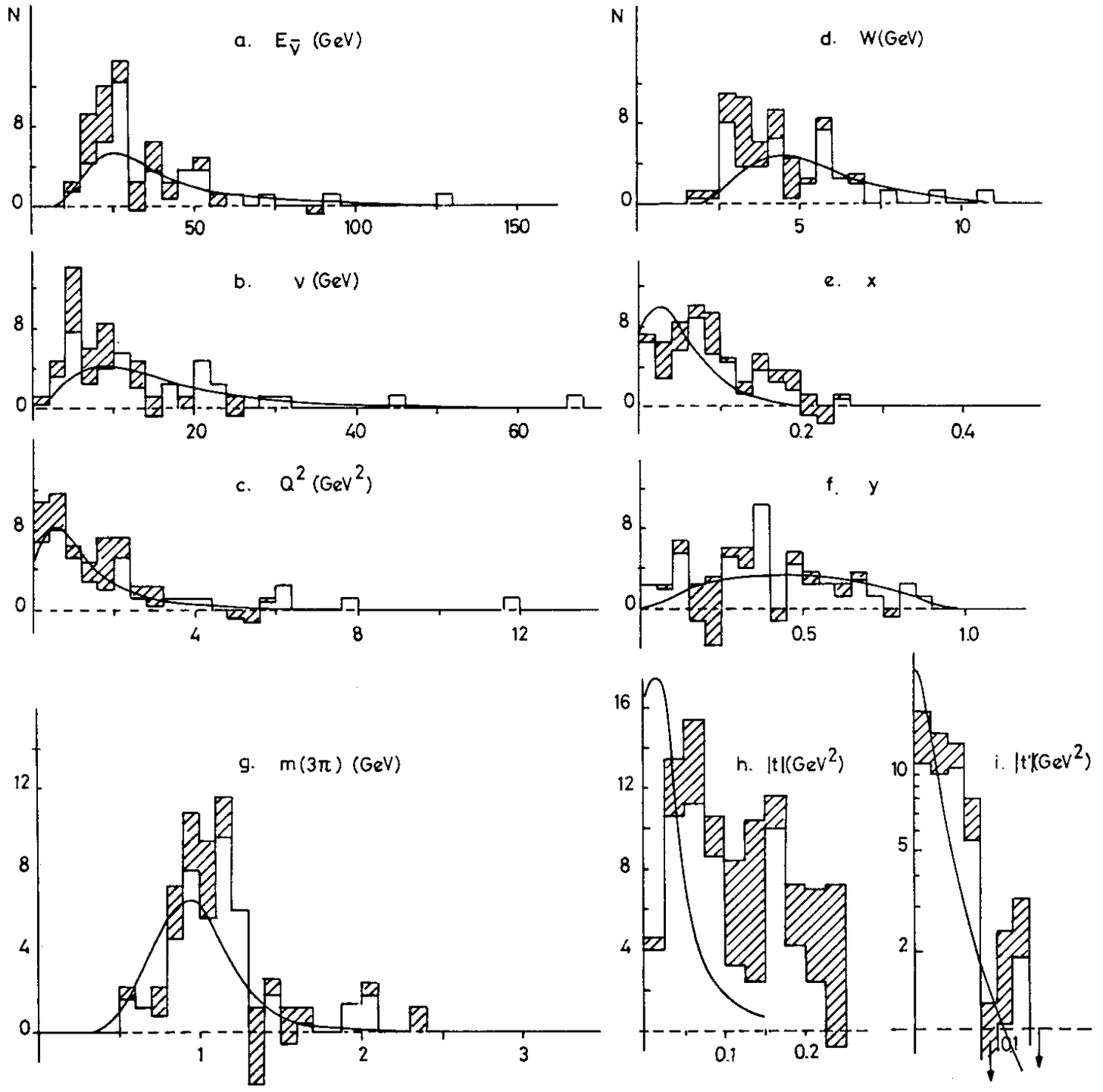
N
a. $E_{\bar{\nu}}$ (GeV)
8
0
50
100
150
b. ν (GeV)
20
40
60
c. Q^2 (GeV^2)
4
8
12
d. W(GeV)
5
10
e. x
0.2
0.4
f. y
0.5
1.0
g. m(3π) (GeV)
12
4
1
2
3
h. |t|(GeV^2)
16
0.1
0.2
i. |t'|(GeV^2)
10
2

Fig. 5